

Low-scale leptogenesis and dark matter in a three-loop radiative seesaw model

Osamu Seto^a, Tetsuo Shindou^b, and Takanao Tsuyuki^{b*}

^a*Department of Physics, Hokkaido University, Sapporo 060-0810, Japan*

^b*Division of Liberal-Arts, Kogakuin University, Hachioji, Tokyo 192-0015, Japan*

Abstract

We show that three open questions in particle physics and cosmology: the origin of neutrino mass, the identity of dark matter, and the origin of the baryon asymmetry of the universe can be explained simultaneously in the three-loop seesaw model proposed by Krauss, Nasri, and Trodden. We discuss the difficulty of successful leptogenesis with three right-handed neutrinos, and we propose a scenario with four right-handed neutrinos that satisfies all observational constraints. This scenario predicts a sleptonlike particle as light as a few hundreds GeV that can be probed by future collider experiments.

EPHOU-22-022, KU-PH-033

1 INTRODUCTION

The observation of neutrino oscillation has confirmed that neutrinos have masses. The neutrino oscillation parameters [1] and the cosmological observations [2] indicate that neutrino masses are many orders of magnitude smaller than those of the other standard model (SM) fermions. We need some mechanism beyond the SM to explain such tiny masses.

When we consider cosmology, there are additional strong motivations to consider the new physics beyond the SM. One is that there is no appropriate candidate for dark matter (DM) in the SM. Another problem is that the baryogenesis does not work in the SM, as the electroweak baryogenesis requires a smaller Higgs boson mass than the observed one.

The canonical seesaw mechanism [3–6] is a favorable idea to address the origin of the neutrino masses, in which neutrino masses are suppressed by heavy right-handed (RH) neutrino masses. In such models, on the one hand, the thermal leptogenesis [7] works as a mechanism of the baryogenesis, where the CP -violating decay of the right-handed neutrino produces the lepton asymmetry, which is partially converted to the baryon asymmetry through the sphaleron process. The disadvantage of the thermal leptogenesis in the seesaw model is that it tends to require a right-handed neutrino to be as heavy as 10^9 GeV [8–10] and cannot be tested by experiments. In addition, further extensions would be necessary because the minimal seesaw model does not contain a suitable candidate for DM.

*tsuyuki@cc.kogakuin.ac.jp

An alternative approach to explain the tininess of the neutrino masses is to utilize loop factors [11–17]. A class of models with right-handed neutrinos, so-called radiative seesaw models, is particularly attractive. In these models, a discrete symmetry under which the right-handed neutrinos and some extra scalars are odd is introduced to forbid the tree-level neutrino-mass generation. This symmetry can also stabilize the lightest odd-charged particle as the DM.

In this paper, we focus on the radiative seesaw model proposed by Krauss, Nasri, and Trodden [15] (often called the KNT model), where tiny neutrino masses are generated via three-loop diagrams. To forbid the tree-level contribution to neutrino masses, a Z_2 symmetry is introduced under which the right-handed neutrinos and a charged scalar S_2 is odd. Therefore, the lightest right-handed neutrino can be a candidate for the DM. The phenomenology of the KNT model has been studied in Refs. [18–23]. In our previous work [23], we have found that the KNT model is severely constrained for the inverted neutrino-mass ordering case by the experiments searching for the lepton flavor violation (LFV). A model proposed by Ma [16] (sometimes called the scotogenic model) also shares properties that neutrino masses are radiatively generated at the one-loop level and possess a dark matter candidate. From the viewpoint of the philosophy of radiative generation of neutrino mass, the KNT model would be more appealing than Ma’s scotogenic model with a TeV scale mass of extra scalars that need a small scalar quartic coupling $\mathcal{O}(10^{-5})$ besides the one-loop suppression factor that is not enough to reduce neutrino masses down to sub-eV scale. Phenomenologically, the DM in the KNT model is a Majorana right-handed neutrino, while that in the scotogenic model is the scalar in a heavier inert doublet Higgs doublet.¹ There are different dark matter phenomenology.

Baryogenesis in the context of the KNT model has been scarcely considered. The high-scale leptogenesis in an extended KNT model has been studied [26] but not for the original KNT model. In the KNT model, the decay of the second lightest right-handed neutrino N_2 into a charged lepton ℓ_R^\mp and S_2^\pm can produce the lepton asymmetry. One difficulty of the leptogenesis in the KNT model is that the asymmetry generated by the N_2 decay is cancelled and washed out² after the decay $S_2^\pm \rightarrow N_1 \ell_R^\pm$. In this paper, we point out that this washout can be suppressed if S_2 is relatively light and its Boltzmann suppression is not strong at the sphaleron freeze-out time. Since the sphaleron freeze-out temperature T_{sph} is about $\simeq 130$ GeV [27], S_2 must be lighter than a few hundreds GeV. The light S_2 behaves like a slepton and can be explored by direct searches at the collider experiments such as the International Linear Collider (ILC) [28,29], the Compact Linear Collider [30], the Future Circular Collider [31], or Circular Electron Positron Collider (CEPC) [32,33]. Another difficulty of the leptogenesis is due to the $\Delta L = 2$ washout processes such as $\ell_i^\pm S_2^\mp \leftrightarrow \ell_j^\mp S_2^\pm$ via exchange of right-handed neutrinos [34,35]. Those washout reaction rates are, in general, many order of magnitude larger than the cosmic expansion rate, hence, the generated lepton asymmetry hardly survive. Thus we may need an extension of the model to explain the baryon asymmetry via leptogenesis. A simple solution is introducing the fourth generation of the right-handed neutrino, and we adopt this possibility in this paper. We check that our scenario of leptogenesis is compatible with the observations such as the neutrino oscillation, the DM abundance, and LFV processes.

¹The case of the lightest right-handed neutrino dark matter is hardly compatible with various experimental results and theoretical consistency [24] or needs fine-tuned mass spectrum so that co-annihilation works [25].

²This problem does not exist in the scotogenic model with scalar DM

This paper is organized as follows. In Sec. 2, we briefly review the KNT model and discuss the constraints from the neutrino oscillation, the lepton flavor violations, the relic abundance of the dark matter, and direct searches of new particles. In Sec. 3, we discuss the possibility of leptogenesis, and we show that the observed baryon asymmetry can be explained in the case of four right-handed neutrinos. In Sec. 4, we summarize this paper and make concluding remarks.

2 The KNT model

2.1 The Lagrangian and the neutrino-mass matrix

We consider the KNT model [15], which explains the tininess of neutrino masses by utilizing the loop factor. In the model, charged scalar fields S_1 and S_2 and RH neutrinos N_I with I are the generation indices are introduced. Furthermore, a global Z_2 symmetry is introduced, under which S_1 and N_I fields are assigned odd and S_2 is assigned even.

This symmetry is necessary to forbid the neutrino Yukawa couplings with the right-handed neutrinos, left-handed lepton doublets, and the Higgs doublet, which would provide too large Dirac neutrino-mass terms after the electroweak symmetry breaking. The Z_2 symmetry simultaneously guarantees the stability of the lightest Z_2 odd particle. If N_1 is the lightest, it can be a DM candidate. The Lagrangian terms added to the SM are

$$\mathcal{L}_{\text{KNT}} = \frac{h_{ij}}{2} \overline{L}_i^c i \tau_2 L_j S_1^+ + g_{Ij}^* \overline{N}_I^c \ell_{Rj} S_2^+ + \frac{m_{N_I}}{2} \overline{N}_I^c N_I + \text{H.c.} - V, \quad (1)$$

where the superscript c denotes the charge conjugation, the Yukawa matrix (h_{ij}) is an antisymmetric, *i.e.*, $h_{ij} = -h_{ji}$, g_{Ij} are other Yukawa coupling constants, λ_S is a complex coupling, and N_I are in the mass basis. The scalar potential V includes four-point scalar coupling terms,

$$V \supset \frac{\lambda_S}{4} (S_1^-)^2 (S_2^+)^2 + \text{H.c.} \quad (2)$$

With the Lagrangian, the neutrino masses are induced through the Feynman diagram in Fig. 1. A component of the neutrino-mass matrix is given by [19]³

$$M_{ab} = \frac{\lambda_S}{4(4\pi)^3 m_{S_1}} \sum_{I,j,k} m_{\ell_j} m_{\ell_k} h_{aj} h_{bk} g_{Ij} g_{Ik} f_I. \quad (3)$$

Here, we use a simple expression for the loop function f_I found in Ref. [23]:

$$\begin{aligned} f_I &= \frac{\sqrt{x_I}}{8y^{3/2}} \int_0^\infty dr \frac{J^2}{r(r+x_I)}, \\ J &= q \ln \left[\frac{y}{q} \right] + \frac{y}{q} \ln[q] + (1+r) \ln \left[\frac{1+r}{y} \right], \\ q &= \frac{1}{2} \left(1+r+y + \sqrt{(1+r+y)^2 - 4y} \right), \\ x_I &= \frac{m_{N_I}^2}{m_{S_2}^2}, \quad y = \frac{m_{S_1}^2}{m_{S_2}^2}. \end{aligned} \quad (4)$$

³Our convention is slightly different from Ref. [19]: $h_{ij} = f_{ij}/2$ and $f_I = \sqrt{y}F(x_I, y)$.

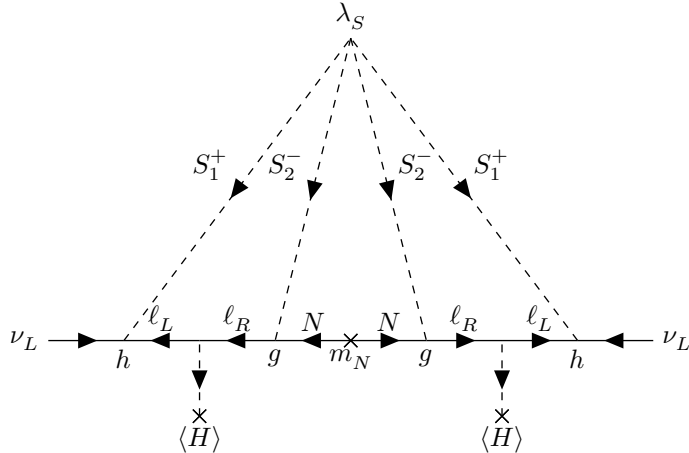


Figure 1: The diagram of the neutrino-mass generation in the KNT model.

As discussed later, since observations constrain $m_{N_1} \lesssim \mathcal{O}(100)$ GeV, $m_{S_1} \gtrsim \mathcal{O}(10^4)$ GeV, and $m_{S_2} \simeq \mathcal{O}(10^2)$ GeV, the region of $y \gg x_1$ and $y \gg 1$ is of interest. In such a case, the loop function can be analytically estimated as

$$f_1 \simeq \frac{\zeta(2) + \zeta(3)}{2} \sqrt{\frac{x_1}{y}} \simeq 1.42 \frac{m_{N_1}}{m_{S_1}}, \quad (5)$$

where ζ is the Riemann zeta function. In Fig. 2, we plot the loop function in the case of $y \gg 1$ and the analytic expression equation (5), and we find that the analytic expression provides a good approximation in the region $m_{N_1} \lesssim 0.1 m_{S_2}$.

To find a parameter set that reproduces the neutrino oscillation data by the mass matrix equation (3), we can use the relations found in Refs. [22, 23]. In Eq. (3), there are terms suppressed by the small electron mass m_e , which can be ignored. Under this approximation, we can extract conditions on h_{ij} as

$$\frac{M_{e\mu}M_{\mu\tau} - M_{e\tau}M_{\mu\mu}}{M_{\mu\mu}M_{\tau\tau} - M_{\mu\tau}^2} = \frac{h_{12}}{h_{23}}, \quad (6)$$

$$\frac{M_{e\mu}M_{\tau\tau} - M_{e\tau}M_{\mu\tau}}{M_{\mu\mu}M_{\tau\tau} - M_{\mu\tau}^2} = \frac{h_{13}}{h_{23}}. \quad (7)$$

2.2 Lepton flavor violation

In the KNT model, the charged lepton flavor is not conserved. Thus, charged leptons ℓ_i can decay into the lighter one ℓ_j and a photon γ . The branching ratio of this process is estimated as [19, 23]

$$\text{Br}(\ell_i \rightarrow \ell_j \gamma) = \frac{48\pi^3 \alpha_{\text{em}}}{G_F^2} \left(|A_L^{ij}|^2 + |A_R^{ij}|^2 \right) \text{Br}(\ell_i \rightarrow \ell_j \nu \bar{\nu}), \quad (8)$$

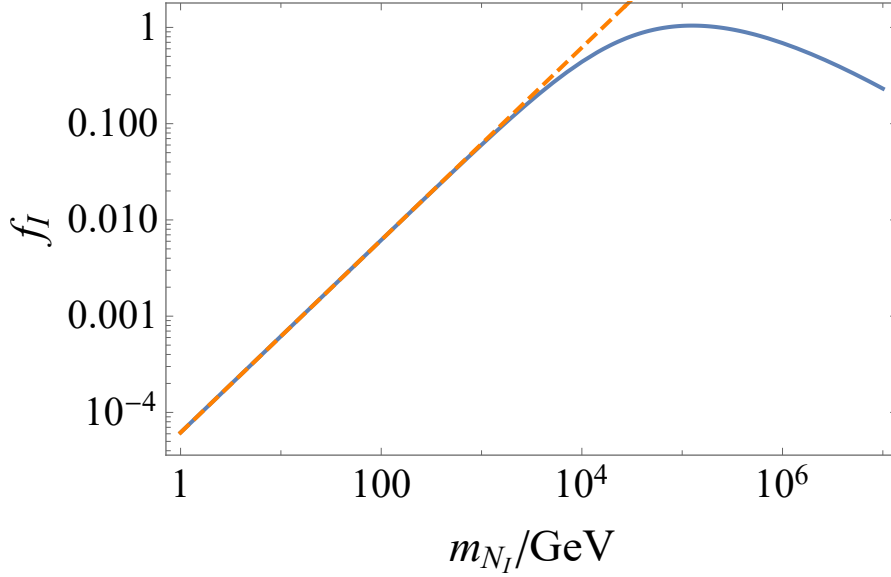


Figure 2: The numerical behavior of the loop function f_I . The blue line shows the loop function f_I in the expression of the neutrino masses in Eq. (3) with $m_{S_1} = 2.3 \times 10^4$ GeV, $m_{S_2} = 100$ GeV. The orange-dashed line shows the analytic approximation given in Eq. (5).

where A_R^{ij} and A_L^{ij} are given by

$$A_R^{ij} = \frac{1}{16\pi^2 m_{S_2}^2} \sum_{I=1}^{n_N} g_{Ii}^* g_{Ij} F_2(x_I), \quad (9)$$

$$A_L^{ij} = \frac{1}{192\pi^2 m_{S_1}^2} h_{il} h_{jl}^* \quad (l \neq i, j),$$

α_{em} is the fine structure constant, and G_F is the Fermi constant. The loop function $F_2(x)$ is defined as [36]⁴

$$F_2(x) = \frac{2x^2 + 5x - 1}{12(x-1)^3} - \frac{x^2 \log(x)}{2(x-1)^4}. \quad (10)$$

The most severe constraint comes from $\mu \rightarrow e\gamma$. The current upper bound on this process is given by $\text{Br}(\mu \rightarrow e\gamma) < 4.2 \times 10^{-13}$ [37]. Even if $A_R^{21} = 0$ is satisfied by taking a specific form for g_{Ii} , A_L^{21} cannot be taken as zero because of the antisymmetric structure of (h_{ij}) . Since $|A_R^{21}|^2 \geq 0$, the branching ratio satisfies

$$\begin{aligned} \text{Br}(\mu \rightarrow e\gamma) &\geq \frac{48\pi^3 \alpha_{\text{em}}}{G_F^2} \left| \frac{h_{23} h_{13}^*}{192\pi^2 m_{S_1}^2} \right|^2 \\ &= 2.22 \times 10^{-14} |h_{23}|^4 \left| \frac{h_{13}}{h_{23}} \right|^2 \left(\frac{10^4 \text{GeV}}{m_{S_1}} \right)^4. \end{aligned} \quad (11)$$

Note that the factor h_{13}/h_{23} is determined by the elements of the neutrino-mass matrix, as shown in Eq. (7).

⁴This function $F_2(x)$ differs from the $F_1(x)$ in Ref. [20] by factor 2, i.e., $F_2(x) = \frac{1}{2}F_1(x)$.

As for neutrino-mass parameters, we input the best-fit values of normal ordering with super-Kamiokande data in Ref. [1]. In the KNT model, the lightest active neutrino mass is zero because of the antisymmetric structure of (h_{ij}) [22]. Hence, the other active neutrino masses are determined by the observed mass-squared differences. In this case, the remaining free parameter in M_{ab} is one Majorana phase. In the following, we set the Majorana phase to zero for simplicity. With a finite value of the Majorana phase, the analysis does not change much. If the neutrino-mass ordering is inverted, the factor $|h_{13}/h_{23}|$ is larger than that of the normal ordering case [22]. The combination of the upper bound on $\text{Br}(\mu \rightarrow e\gamma)$ and the perturbativity condition was studied in Ref. [23], and inverted ordering is severely constrained.

By inputting the neutrino oscillation data and the upper bound of $\text{Br}(\mu \rightarrow e\gamma)$ to Eq.(11), we obtain the lower bound on m_{S_1} :

$$m_{S_1} > 8700|h_{23}| \text{ GeV}. \quad (12)$$

2.3 Slepton searches

In the KNT model, S_2 behaves like a purely right-handed slepton in supersymmetric models. In the case considered below ($g_{11} = g_{12} = 0$), it is like a right-handed stau $\tilde{\tau}_R$. The mass bounds on $\tilde{\tau}_R$ are obtained by the LEP experiments [38–42].⁵ The bounds come from the search for the stau decay ($S_2 \rightarrow \tau + N_1$ in our case) and they depend on m_{N_1} . In the exclusion plot in Ref. [44], the strongest bound is $m_{S_2} \gtrsim 95.5 \text{ GeV}$ (95% confidence level) at $m_{N_1} \simeq 64 \text{ GeV}$. In the analysis below, we use a conservative bound

$$m_{S_2} > 96 \text{ GeV} \quad (13)$$

for all the m_{N_1} region.

2.4 Dark matter

The lightest right-handed neutrino N_1 is stabilized by the Z_2 symmetry and it can be the dark matter. We assume that N_1 was produced as thermal relics. The abundance of such dark matter is determined by the annihilation cross section. Since the dark matter mass m_{N_1} cannot be very large, we naively expect to have a significant contribution to the LFV via S_2 and N_1 exchange diagrams. To avoid such a contribution, it is preferred that N_1 couples to only one lepton flavor. Thus, we here make an ansatz that N_1 only couples to τ , i.e., $g_{11} = g_{12} = 0$ and $g_{13} \neq 0$. With this ansatz, the cross section is calculated as [15, 18, 19]

$$\langle\sigma v\rangle \simeq \frac{m_{N_1}^2(m_{N_1}^4 + m_{S_2}^4)}{8\pi(m_{N_1}^2 + m_{S_2}^2)^4} |g_{13}|^4 \frac{1}{x_f}, \quad (14)$$

with $x_f \simeq 20$ [45]. The relic abundance of the dark matter after the decoupling is approximated by

$$\Omega_{N_1} h^2 \simeq 0.12 \frac{2.9 \times 10^{-9} \text{ GeV}^{-2}}{\langle\sigma v\rangle}. \quad (15)$$

⁵In the analysis by the CMS Collaboration [43], constraints on the degenerate or purely left-handed stau were obtained. However, they note that their sensitivity for the purely right-handed stau was insufficient and the constraint was not available.

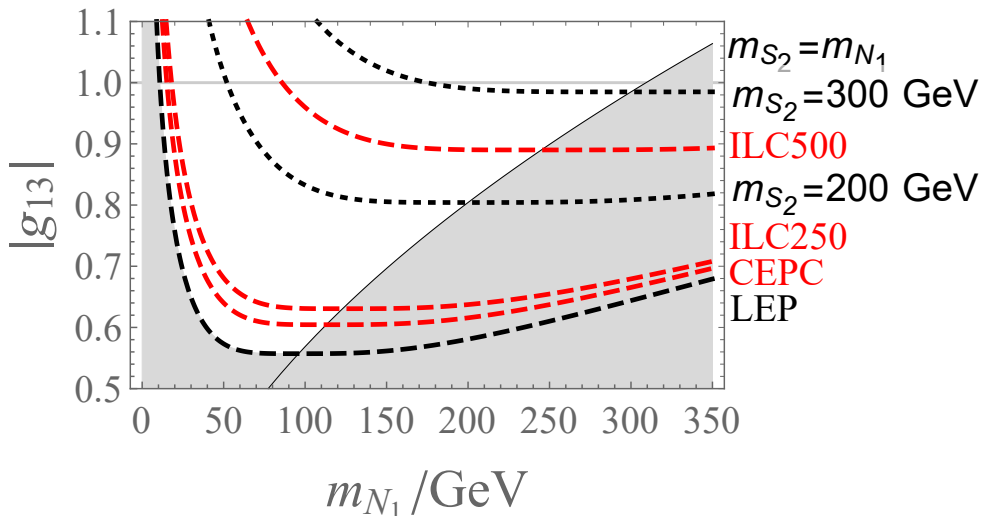


Figure 3: Contour of m_{S_2} in the plane of the dark matter mass m_{N_1} and its Yukawa coupling $|g_{13}|$. The white region satisfies conditions to explain dark matter and leptogenesis. The black-dashed curve shows the simplified lower bound from LEP ($m_{S_2} > 96$ GeV) [44] and red-dashed curves show the simplified sensitivity up limit on m_{S_2} of future experiments (CEPC: 113 GeV [33], ILC250: 123 GeV, ILC500: 245 GeV [29]). The dotted lines are contours of $m_{S_2} = 200$ GeV, 300 GeV. These curves are obtained by using the DM condition equation (16). The right-bottom shaded corner is the region where the charged S_2 is lighter than N_1 . The horizontal-gray line shows the perturbativity up limit.

By comparing the observed dark matter abundance $\Omega_{N_1} h^2 = 0.120 \pm 0.001$ [2], we obtain

$$|g_{13}| \simeq 0.35 \frac{x_1 + 1}{[x_1(x_1^2 + 1)]^{1/4}} \left(\frac{m_{S_2}}{100 \text{ GeV}} \right)^{1/2}, \quad (16)$$

where $x_1 = m_{N_1}^2/m_{S_2}^2$.

In Fig. 3, we show the contour of m_{S_2} in the m_{N_1} - $|g_{13}|$ plane which can reproduce the thermal relic abundance of the DM. By the perturbativity condition $|g_{13}| \leq 1$, there is a lower and upper bound on the dark matter mass m_{N_1} :

$$11 \text{ GeV} < m_{N_1} < 310 \text{ GeV}. \quad (17)$$

The upper bound gives

$$m_{S_2} < 310 \text{ GeV}. \quad (18)$$

As discussed later, m_{S_2} less than $\mathcal{O}(100)$ GeV is also preferred to explain the baryon asymmetry by the leptogenesis.

2.5 The minimal case

We here consider the minimal structure of (g_{Ii}) to explain both the neutrino mixing and the dark matter with satisfying the lepton flavor violation constraints.

To explain the neutrino oscillation data, we should reproduce $M_{\tau\tau}$, $M_{\mu\mu}$, and $M_{\mu\tau}$. Once these elements are reproduced, the other elements can be tuned by h_{12}/h_{23} and h_{13}/h_{23} . To realize it, we need at least three independent g_{Ij} . On the other hand, the elements g_{I1} are irrelevant to the neutrino-mass matrix because of the strong suppression by m_e . Therefore, we need at least two RH neutrinos which have a significant size of the Yukawa coupling with μ and/or τ . If we use N_1 and N_3 for generating an appropriate neutrino mass matrix,⁶ g_{32} and g_{33} should have significant size, as $g_{22} = 0$ is taken in Sec. 2.4. In addition, g_{31} should be small to avoid too large a contribution to $\mu \rightarrow e\gamma$ through the S_2 exchange diagrams. Thus, the minimal setup of the Yukawa couplings with $\overline{N}_I^c \ell_{Ri} S_2^+$ for the neutrino mixing and the dark matter is given by

$$\mathcal{L} = (\overline{N}_1^c \quad \overline{N}_3^c) \begin{pmatrix} 0 & 0 & g_{13}^* \\ 0 & g_{32}^* & g_{33}^* \end{pmatrix} \begin{pmatrix} e_R \\ \mu_R \\ \tau_R \end{pmatrix} S_2^+ + \text{h.c.} . \quad (19)$$

With the setup, three components of the neutrino-mass matrix in Eq. (3) become

$$M_{\mu\mu} = \frac{\lambda_S m_\tau^2 h_{23}^2}{4(4\pi)^3 m_{S_1}} (g_{13}^2 f_1 + g_{33}^2 f_3) , \quad (20)$$

$$M_{\mu\tau} = -\frac{\lambda_S m_\mu m_\tau h_{23}^2}{4(4\pi)^3 m_{S_1}} g_{32} g_{33} f_3 , \quad (21)$$

$$M_{\tau\tau} = \frac{\lambda_S m_\mu^2 h_{23}^2}{4(4\pi)^3 m_{S_1}} g_{32}^2 f_3 , \quad (22)$$

and we can see that there are enough degrees of freedom to reproduce an appropriate neutrino matrix. Note that the inverted ordering case with the best-fit oscillation parameters is excluded by the $\mu \rightarrow e\gamma$ constraint.⁷ Thus, we consider the normal ordering case throughout this paper.

Let us comment on the lepton flavor violation processes other than $\mu \rightarrow e\gamma$. If the constraint (12) is satisfied, the contribution of S_1 to the other decays $\tau \rightarrow e\gamma$ and $\tau \rightarrow \mu\gamma$ is the same order as $\mu \rightarrow e\gamma$ and much weaker than the experimental constraints. In our case of $g_{I1} = 0$, S_2 does not contribute to $\mu \rightarrow e\gamma$ and $\tau \rightarrow e\gamma$. On the other hand, the S_2 contribution to $\tau \rightarrow \mu\gamma$ is given as

$$\text{Br}(\tau \rightarrow \mu\gamma) \simeq \frac{48\pi^3 \alpha_{em}}{G_F^2} \left| \frac{g_{32}^* g_{33}}{16\pi^2 m_{S_2}^2} F_2(x_3) \right|^2 \text{Br}(\tau \rightarrow \mu\nu\bar{\nu}) . \quad (23)$$

Using the upper bound $\text{Br}(\tau \rightarrow \mu\gamma) < 4.2 \times 10^{-8}$ [46] and $\text{Br}(\tau \rightarrow \mu\nu\bar{\nu}) = 0.1739$ [47], we find

$$|g_{32} g_{33}| F_2(x_3) < 2.7 \times 10^{-3} \left(\frac{m_{S_2}}{100 \text{ GeV}} \right)^2 . \quad (24)$$

3 Leptogenesis

3.1 Production and evolutions of the asymmetry

For baryogenesis, we consider a scenario that the CP -violating decay of N_2 to ℓ_R and S_2 generates the lepton asymmetry, and the lepton asymmetry is converted to the baryon asym-

⁶As discussed in Sec. 3, N_2 will be necessary for the leptogenesis, and the mass m_{N_2} is required to be smaller than m_{N_3} . So that we here use N_3 instead of N_2 .

⁷It corresponds to the $n_{\text{eff}} = 1$ case in Ref. [23].

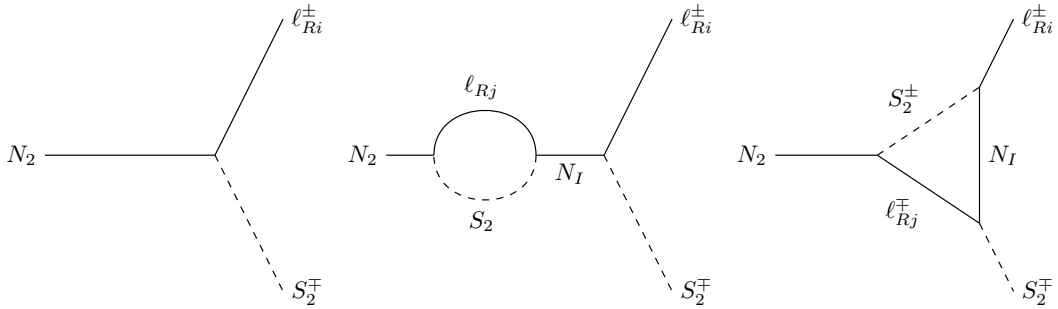


Figure 4: The Feynman diagrams relevant to the CP asymmetric decay of $N_2 \rightarrow \ell_R S_2$ at the one-loop level.

metry by the sphaleron process. The CP asymmetry in the decay $N_2 \rightarrow \ell_{Ri}^{\pm} S_2^{\mp}$ is defined as

$$\epsilon_i \equiv \frac{\Gamma(N_2 \rightarrow \ell_{Ri}^- S_2^+) - \Gamma(N_2 \rightarrow \ell_{Ri}^+ S_2^-)}{\Gamma(N_2 \rightarrow \ell_{Ri}^- S_2^+) + \Gamma(N_2 \rightarrow \ell_{Ri}^+ S_2^-)}, \quad (25)$$

which comes from the interference between the tree diagram and the loop diagrams shown in Fig. 4.

For producing enough large lepton asymmetry, the decay width of N_2 should not be too large compared to the Hubble rate at around $T = m_{N_2}$. To examine this, we define K as the ratio of the total decay width of N_2 , $\Gamma_{N_2} = \Gamma(N_2 \rightarrow \ell_R^+ S_2^-) + \Gamma(N_2 \rightarrow \ell_R^- S_2^+)$ and the Hubble rate H at $T = m_{N_2}$ [45]:

$$K \equiv \frac{\Gamma_{N_2}}{2H} \Big|_{T=m_{N_2}} = \frac{\sum_i |g_{2i}|^2}{8\pi} m_{N_2} \times \left(\frac{8\pi^3 g_*}{90} \right)^{-\frac{1}{2}} \frac{M_P}{m_{N_2}^2} = 2.8 \times 10^{13} \sum_i |g_{2i}|^2 \frac{10^3 \text{ GeV}}{m_{N_2}}, \quad (26)$$

where $g_* = 110.5$ is the effective relativistic degrees of freedom by taking into account S_2 , N_1 , and N_2 , and $K \lesssim 1$ is required. To realize it, the Yukawa couplings g_{2i} should be too strongly suppressed for N_2 to contribute to the neutrino-mass matrix. Thus N_2 should be introduced in addition to N_1 and N_3 .

We consider the chemical potentials before the sphaleron freeze-out to derive the relation between the baryon number and the lepton number in our model. We denote the chemical potentials by μ and subscripts q, u, d, L, ℓ_R, ϕ indicate the SM quark doublet, right-handed up-type quark, right-handed down-type quark, lepton doublet, right-handed charged lepton, and the Higgs doublet. The chemical potential of the Majorana particles is zero $\mu_N = 0$. The SM Yukawa interactions and the sphaleron process yields⁸

$$-\mu_q - \mu_\phi + \mu_u = 0, \quad (27)$$

$$-\mu_q + \mu_\phi + \mu_d = 0, \quad (28)$$

$$-\mu_L + \mu_\phi + \mu_{\ell_R} = 0, \quad (29)$$

$$3\mu_q + \mu_L = 0. \quad (30)$$

⁸We ignore the effects of the top quark decoupling and phase transition near the sphaleron freeze-out temperature.

The conditions from vanishing hypercharge in the Universe and the non-SM interaction are [26]

$$3(\mu_q - \mu_d + 2\mu_u - \mu_L - \mu_{\ell_R}) + 2(\mu_\phi + \mu_{S_2}) = 0, \quad (31)$$

$$\mu_{S_2} + \mu_{\ell_R} = 0. \quad (32)$$

These equations can be solved as

$$\begin{aligned} \mu_q &= -\frac{8}{9}\mu_{\ell_R}, \quad \mu_u = \frac{7}{9}\mu_{\ell_R}, \quad \mu_d = -\frac{23}{9}\mu_{\ell_R}, \\ \mu_L &= \frac{8}{3}\mu_{\ell_R}, \quad \mu_\phi = \frac{5}{3}\mu_{\ell_R}, \quad \mu_{S_2} = -\mu_{\ell_R}. \end{aligned} \quad (33)$$

Now, the condition (39) becomes clear. If the condition is not satisfied, it ends up with $\mu_{S_2} = -\mu_{\ell_R} = 0$. The relation of the baryon number $B = 3 \times 3 \times (1/3) \times (2\mu_q + \mu_u + \mu_d)$ and the lepton number $L = \sum_i (\mu_{L_i} + \mu_{\ell_{Ri}})$ is expressed as

$$B = \frac{32}{79}(B - L). \quad (34)$$

The sets of Boltzmann equations to be solved are those of N_2, ℓ_i and S_2^\pm . Those are rewritten as the Boltzmann equations for the number density of N_2 and asymmetries of number densities of $B/3 - L_i$ and $S_2^+ - S_2^-$, respectively, as (n_X denotes the number density

of the species X)

$$\begin{aligned}
\frac{dn_{N_2}}{dt} + 3Hn_{N_2} = & - \sum_i \langle \Gamma(N_2 \rightarrow S_2^\pm \ell_i^\mp) \rangle (n_{N_2} - n_{N_2}^{\text{eq}}) \\
& - \sum_{i,j} \langle \sigma v(N_2 N_1 \leftrightarrow \ell_i^\mp \ell_j^\pm) \rangle (n_{N_2} n_{N_1} - n_{N_2}^{\text{eq}} n_{N_1}^{\text{eq}}) \\
& - \sum_{i,j} \langle \sigma v(N_2 \ell_i^\mp \leftrightarrow \ell_j^\mp N_1) \rangle (n_{N_2} n_{\ell_i^\mp} - n_{N_2}^{\text{eq}} n_{\ell_i^\mp}^{\text{eq}}), \tag{35}
\end{aligned}$$

$$\begin{aligned}
\frac{dn_{B/3-L_i}}{dt} + 3Hn_{B/3-L_i} = & - \epsilon_i \langle \Gamma(N_2 \rightarrow S_2^\pm \ell_i^\mp) \rangle (n_{N_2} - n_{N_2}^{\text{eq}}) \\
& - \langle \Gamma(S_2^+ \ell_i^- \rightarrow N_2) \rangle n_{B/3-L_i} - \langle \Gamma(S_2^+ \ell_i^- \rightarrow N_2) \rangle n_{S_2^+ - S_2^-} \\
& + \langle \Gamma(S_2^+ \rightarrow N_1 \ell_i^+) \rangle n_{S_2^+ - S_2^-} - \frac{1}{2} \langle \Gamma(N_1 \ell_i^+ \rightarrow S_2^+) \rangle n_{B/3-L_i} \\
& - \sum_j \langle \sigma v(\ell_i^- \ell_j^- \leftrightarrow S_2^- S_2^-) \rangle \left(\frac{n_{\ell_i^- + \ell_j^-}}{2} n_{B/3-L_j} + \frac{n_{\ell_j^- + \ell_i^-}}{2} n_{B/3-L_i} \right) \\
& + \sum_j \langle \sigma v(\ell_i^+ \ell_j^+ \leftrightarrow S_2^+ S_2^+) \rangle n_{S_2^+ + S_2^-} n_{S_2^+ - S_2^-} \\
& + \sum_j \langle \sigma v(\ell_i^- S_2^+ \leftrightarrow \ell_j^+ S_2^-) \rangle \left(\frac{n_{\ell_i^- + \ell_j^+}}{2} n_{S_2^+ - S_2^-} - \frac{n_{S_2^+ + S_2^-}}{2} n_{B/3-L_i} \right) \\
& + \sum_j \langle \sigma v(\ell_i^+ S_2^- \leftrightarrow \ell_j^- S_2^+) \rangle \left(\frac{n_{\ell_j^- + \ell_i^+}}{2} n_{S_2^+ - S_2^-} - \frac{n_{S_2^+ + S_2^-}}{2} n_{B/3-L_j} \right), \tag{36}
\end{aligned}$$

$$\begin{aligned}
\frac{dn_{S_2^+ - S_2^-}}{dt} + 3Hn_{S_2^+ - S_2^-} = & \sum_i \epsilon_i \langle \Gamma(N_2 \rightarrow S_2^\pm \ell_i^\mp) \rangle (n_{N_2} - n_{N_2}^{\text{eq}}) \\
& + \sum_i \langle \Gamma(S_2^+ \ell_i^- \rightarrow N_2) \rangle n_{S_2^+ - S_2^-} + \sum_i \langle \Gamma(S_2^+ \ell_i^- \rightarrow N_2) \rangle n_{B/3-L_i} \\
& - \sum_i \langle \Gamma(S_2^+ \rightarrow N_1 \ell_i^+) \rangle n_{S_2^+ - S_2^-} + \sum_i \frac{1}{2} \langle \Gamma(N_1 \ell_i^+ \rightarrow S_2^+) \rangle n_{B/3-L_i} \\
& + \sum_{i,j} \langle \sigma v(\ell_i^- \ell_j^- \leftrightarrow S_2^- S_2^-) \rangle \left(\frac{n_{\ell_i^- + \ell_j^-}}{2} n_{B/3-L_j} + \frac{n_{\ell_j^- + \ell_i^-}}{2} n_{B/3-L_i} \right) \\
& - \sum_{i,j} \langle \sigma v(\ell_i^+ \ell_j^+ \leftrightarrow S_2^+ S_2^+) \rangle n_{S_2^+ + S_2^-} n_{S_2^+ - S_2^-} \\
& - \sum_{i,j} \langle \sigma v(\ell_i^- S_2^+ \leftrightarrow \ell_j^+ S_2^-) \rangle \left(\frac{n_{\ell_i^- + \ell_j^+}}{2} n_{S_2^+ - S_2^-} - \frac{n_{S_2^+ + S_2^-}}{2} n_{B/3-L_i} \right) \\
& - \sum_{i,j} \langle \sigma v(\ell_i^+ S_2^- \leftrightarrow \ell_j^- S_2^+) \rangle \left(\frac{n_{\ell_j^- + \ell_i^+}}{2} n_{S_2^+ - S_2^-} - \frac{n_{S_2^+ + S_2^-}}{2} n_{B/3-L_j} \right), \tag{37}
\end{aligned}$$

where $\langle \Gamma \rangle$ and $\langle \sigma v \rangle$ are thermal averaged decay (inverse decay) rates and thermal averaged scattering cross section times relative velocity, respectively.

It is a kind of thermal leptogenesis but has some remarkable features. First, the sum of $B - L$ asymmetry and the asymmetry between S_2^+ and S_2^- is always zero, i.e. $\sum_i n_{B/3-L_i} + n_{S_2^+ - S_2^-} = 0$, which is nothing but the electric charge neutrality of the Universe. If S_2 becomes nonrelativistic and decouples from the thermal equilibrium before the sphaleron freeze-out, the abundance of S_2 gets Boltzmann suppressed and the lepton asymmetry is washed out. However, after the sphaleron decouples from the thermal bath at the temperature $T_{\text{sph}} = 131.7 \pm 2.3$ GeV [27], the baryon asymmetry n_B/s is not washed out anymore, while $B - L$ asymmetry is decreasing. With Eq. (34), the final baryon asymmetry is given by

$$\frac{n_B}{s} = \frac{32}{79} \frac{n_{B-L}}{s} \Big|_{T=T_{\text{sph}}}. \quad (38)$$

We stress that the out-of-equilibrium condition for successful baryogenesis in this scenario is satisfied by the sphaleron decoupling. It is different from the situation in the canonical leptogenesis. As a consequence of the behavior, the mass of S_2 should not be much larger than T_{sph} , so that

$$m_{S_2} < \mathcal{O}(100) \text{ GeV}. \quad (39)$$

Second, we discuss the strong washout effect of the scattering process. $\Delta L = 2$ washout processes $\ell_i^\pm S_2^\mp \leftrightarrow \ell_j^\mp S_2^\pm$ and $\ell_i^\pm \ell_j^\pm \leftrightarrow S_2^\pm S_2^\pm$ via N_I exchange are, in general, very strong [34]. Those cross sections are of the order of $\langle \sigma v \rangle \sim |g_{Ii}^* g_{Ij}|^2 / T^2$. The interaction rate $\Gamma \sim T^3 \langle \sigma v \rangle$ is much larger than the Hubble parameter $H \sim T^2 / M_P$ where $M_P = 1.22 \times 10^{19}$ GeV is the Planck mass. This means that the $\Delta L = 2$ washout is very strong unless involved g are extremely small. Since the strength of $\Delta L = 2$ washout are flavor dependent, we need to evaluate lepton asymmetry in each flavor. To reproduce the observed neutrino mixing in the KNT model, g_{32} and g_{33} cannot be small, so that the μ and τ asymmetries are strongly washed out. Producing e asymmetry by the CP -violating decay of $N_2 \rightarrow e_R^\pm S_2^\mp$ is only the possibility. The CP -violating parameter of $N_2 \rightarrow e S_2$ decay is evaluated as

$$\epsilon_1 = \frac{1}{4\pi} \sum_{i=3,4} \frac{\text{Im}[(gg^\dagger)_{2i}^2]}{(gg^\dagger)_{11}} F(m_{N_i}^2 / m_{N_2}^2), \quad (40)$$

$$F(x) \equiv x^{1/2} \left(1 + (1+x) \ln \frac{x}{1+x} + \frac{1}{1-x} \right).$$

In order to produce e asymmetry in the model with three RH neutrinos, a significant size of g_{31} is required to provide the large CP violation in $N_2 \rightarrow e_R^\pm S_2^\mp$ decay. However, such a large g_{31} is disfavored not only by the $\mu \rightarrow e\gamma$ constraint but also by the strong washout effect via the flavor changing $\Delta L = 2$ scattering $e^\pm S_2^\mp \leftrightarrow \ell_i^\mp S_2^\pm$ ($\ell_i = \mu, \tau$). In fact, we cannot find any point which reproduces enough large baryon asymmetry in the case with three RH neutrinos.

A simple extension to solve the above difficulty is introducing the fourth RH neutrino N_4 . The neutrino-mass matrix and the properties of the DM can be explained by N_1 and N_3 , while N_2 and N_4 play an important role in the leptogenesis. In the case that N_2 and N_4 only couple to an electron, ϵ_1 can be enhanced by large g_{41} , while the contribution to $\mu \rightarrow e\gamma$ via N_4 and N_2 exchange and the washout by the flavor changing $\Delta L = 2$ scattering processes are absent.

3.2 Benchmark inputs

We construct a benchmark scenario to demonstrate how the baryon asymmetry is produced in our leptogenesis scenario. With the four RH neutrinos, the Yukawa matrix g is a 4×3 matrix. The minimal structure for the successful leptogenesis is given by

$$g = \begin{pmatrix} 0 & 0 & g_{13} \\ g_{21} & 0 & 0 \\ 0 & g_{32} & g_{33} \\ g_{41} & 0 & 0 \end{pmatrix}. \quad (41)$$

With this structure, there are nine complex and six real parameters:

$$\begin{aligned} \text{complex : } & \lambda_S, h_{12}, h_{13}, h_{23}, g_{13}, g_{21}, g_{32}, g_{33}, g_{41} \\ \text{real : } & m_{S_1}, m_{S_2}, m_{N_1}, m_{N_2}, m_{N_3}, m_{N_4}. \end{aligned} \quad (42)$$

These parameters have to satisfy the neutrino-mass conditions, Eqs. (6), (7), (20), (21), and (22), and two more conditions, i.e., leptogenesis and the DM conditions. The four inequalities (12), (24), (13), and (39), and the perturbativity condition (couplings have to be smaller than the order of unity) must also be obeyed.

In our analysis, we scan m_{N_2} and m_{S_2} in the range of [100, 330] GeV, and we fix the other parameters to satisfy the conditions obtained from the DM relic abundance and neutrino oscillation data. First, we consider the DM relic abundance. Once $|g_{13}|$ and m_{S_2} are fixed, m_{N_1} is determined to reproduce the relic abundance of the DM as shown in Fig. 3. For example, $m_{S_2} = 110$ GeV and $g_{13} = 1.0$ give $m_{N_1} = 12$ GeV.

Second, we take into account the neutrino oscillation data. For the neutrino-mass parameters, we input the best-fit neutrino oscillation parameters in the case with super-Kamiokande data [1]. Once we fix $h_{23} = 1$, Eqs. (6) and (7) determine the rest of the h_{ij} as

$$h_{12} = 0.600e^{-0.0480i}, \quad h_{13} = 0.329e^{0.102i}. \quad (43)$$

We additionally fix $\lambda_S = |g_{32}| = 1$. By using the neutrino-mass equations. (20), (21), and (22) and the approximation formula (5) of f_1 , we obtain

$$M_{\mu\mu} - \frac{M_{\mu\tau}^2}{M_{\tau\tau}} = \frac{1.42m_\tau^2 m_{N_1}}{4(4\pi)^3 m_{S_1}^2} g_{13}^2, \quad (44)$$

$$M_{\tau\tau} = \frac{m_\mu^2}{4(4\pi)^3 m_{S_1}} g_{32}^2 f_3, \quad (45)$$

$$\frac{M_{\mu\tau}}{M_{\tau\tau}} = -\frac{m_\tau g_{33}}{m_\mu g_{32}}. \quad (46)$$

These equations have a solution

$$\begin{aligned} g_{13} &= 1.0, \quad g_{32} = 1.0, \quad g_{33} = -0.053, \\ m_{S_1} &= 2.33 \times 10^4 \text{ GeV}, \quad m_{N_3} = 3.67 \times 10^6 \text{ GeV}. \end{aligned} \quad (47)$$

The branching ratios of the LFV decays in the benchmark point are evaluated as

$$\text{Br}(\mu \rightarrow e\gamma) = 8.2 \times 10^{-17}, \quad (48)$$

$$\text{Br}(\tau \rightarrow \mu\gamma) = 7.5 \times 10^{-15}, \quad (49)$$

Table 1: Definition of benchmark inputs.

Parameter	Value
m_{S_1}	2.33×10^4 GeV
m_{S_2}	Scanned in [100, 330] GeV
m_{N_1}	Depending on m_{S_2}
m_{N_2}	Scanned in [100, 330] GeV
m_{N_3}	3.67×10^6 GeV
m_{N_4}	1.0×10^8 GeV
λ_S	1.0
(h_{12}, h_{23}, h_{13})	$(0.600e^{-0.0480i}, 1.0, 0.329e^{0.102i})$
$(g_{13}, g_{32}, g_{33}, g_{41})$	$(1.0, 1.0, -0.053, 0.1)$
$ g_{21} $	Depending on m_{N_2}
$\arg(g_{21})$	$\pi/4$

which are far below the current limits.

Finally, we fix the rest of the parameters relevant to the leptogenesis. For optimizing the production of the lepton asymmetry, we tune the value of $|g_{21}|$ to satisfy $K = 1$ in Eq. (26) *i.e.*,

$$|g_{21}| = 1.9 \times 10^{-7} \left(\frac{m_{N_2}}{10^3 \text{ GeV}} \right)^{1/2}, \quad (50)$$

and we take $\arg(g_{21}) = \pi/4$ which maximize the CP asymmetry ϵ_1 . We fix the m_{N_4} and g_{41} as $m_{N_4} = 1.0 \times 10^8$ GeV and $g_{41} = 0.1$, respectively. Our benchmark inputs are summarized in Table 1.

3.3 Numerical analysis

We show, in Fig. 5, the evolution of absolute values of asymmetry yield $Y \equiv |n_i|/s$ of each leptons with bluish (dotted) dashed curves, that of $S_2^+ - S_2^-$ with the green curve, that of N_2 with the orange curve, in the case with $m_{S_2} = 110$ GeV and $m_{N_2} = 250$ GeV. The asymmetry of the N_2 decay rates ϵ_1 is [48]: which reflects the charge neutrality, as mentioned above. The total $B - L$ asymmetry drawn with the black dashed curve always coincides with that of $S_2^+ - S_2^-$ asymmetry. We can see that both the total $B - L$ asymmetry and the S_2^\pm asymmetry decreases for a large m_{N_2}/T . At $T = T_{\text{sph}}$, the baryon asymmetry is frozen out as $Y_B = Y_{B-L}|_{T=T_{\text{sph}}}$ due to the sphaleron decoupling. Figure 5 shows that enough large baryon asymmetry $Y_B = \mathcal{O}(10^{-10})$ is obtained in our benchmark.

In Fig. 6, we show an example of contour plots of the final baryon asymmetry for a set of Yukawa coupling constants. The range $m_{S_2} < 310$ GeV is preferred by the DM relic abundance as shown in Fig. 3 and it can be explored by future e^+e^- collider experiments. For example, the CEPC can probe it up to 113 GeV [33], and the ILC with the center of mass energy of 250 GeV can do up to 123 GeV [29]. The Compact Linear Collider with 380 GeV or the ILC with 500 GeV can explore our predicted mass range.

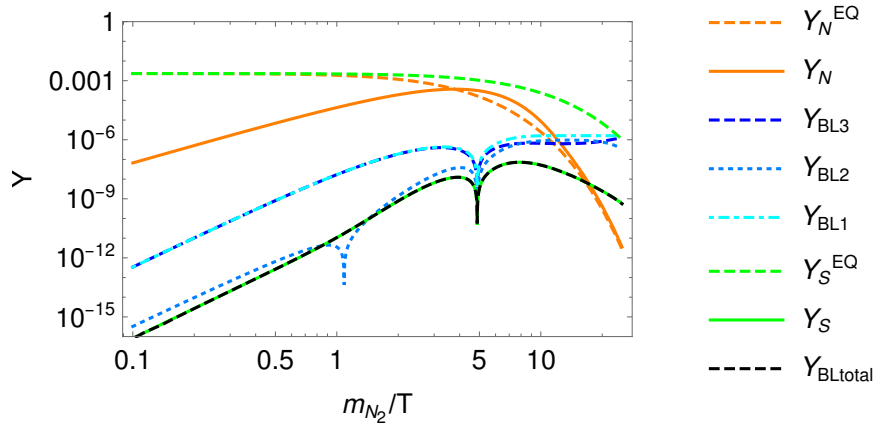


Figure 5: The evolution of yields of each species indicated by the subscriptions: N , BL_i , S , BL_{total} label yields of N_2 , $B/3 - L_i$, S_2 , $B - \sum_i L_i$, respectively. The superscript “EQ” indicates that the line is in thermal equilibrium. The yields are calculated by the Boltzmann equations with the parameters $m_{S_2} = 110$ GeV, $m_{N_2} = 250$ GeV, and the other parameters are shown in Table 1.

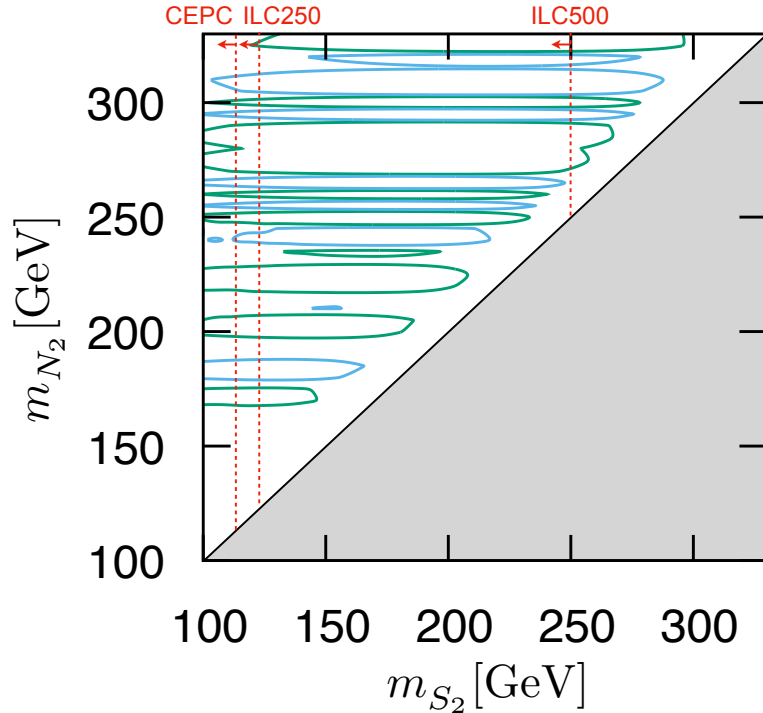


Figure 6: Contours of the yield $Y_B := n_B/s$ for a given set of Yukawa coupling and the CP violation in the m_{S_2} - m_{N_2} plain. Inside of the blue lines is the region of $Y_B > 10^{-10}$ and inside of the green lines gives $Y_B < -10^{-10}$. The vertical-dashed lines show the sensitivities of future experiments: CEPC, ILC at $\sqrt{s} = 250$ GeV and $\sqrt{s} = 500$ GeV.

4 Summary

In this paper, we have proved that neutrino masses, dark matter, and leptogenesis can be explained in the KNT model with four right-handed neutrinos. We have shown explicit parameters that can realize these phenomena and satisfy the observational constraints, such as the LFV decays. To avoid the severe constraint from the LFV decay on the inverted mass ordering case [23], we considered the normal ordering case. In our scenario, there is a definite prediction that a charged scalar particle S_2 should be as light as $m_{S_2} < \mathcal{O}(100)$ GeV. The S_2 in our scenario behaves as a stau-like particle, and it can be detected by future lepton collider experiments.

Acknowledgments

The authors are grateful to Takashi Toma for valuable comments. This work is supported in part by the Japan Society for the Promotion of Science (JSPS) KAKENHI Grants No. 20H00160 (T.S.), Grants No. JP19K03860, No. JP19K03865, No. 23K03402 and MEXT KAKENHI Grant No. 21H00060 (O.S.).

References

- [1] I. Esteban, M. C. Gonzalez-Garcia, M. Maltoni, T. Schwetz, and A. Zhou, “The fate of hints: updated global analysis of three-flavor neutrino oscillations,” *JHEP* **09** (2020) 178, [arXiv:2007.14792 \[hep-ph\]](#).
- [2] **Planck** Collaboration, N. Aghanim *et al.*, “Planck 2018 results. VI. Cosmological parameters,” *Astron. Astrophys.* **641** (2020) A6, [arXiv:1807.06209 \[astro-ph.CO\]](#). [Erratum: *Astron. Astrophys.* 652, C4 (2021)].
- [3] P. Minkowski, “ $\mu \rightarrow e\gamma$ at a Rate of One Out of 10^9 Muon Decays?,” *Phys. Lett. B* **67** (1977) 421–428.
- [4] T. Yanagida, “Horizontal gauge symmetry and masses of neutrinos,” *Conf. Proc. C* **7902131** (1979) 95–99.
- [5] M. Gell-Mann, P. Ramond, and R. Slansky, “Complex Spinors and Unified Theories,” *Conf. Proc. C* **790927** (1979) 315–321, [arXiv:1306.4669 \[hep-th\]](#).
- [6] R. N. Mohapatra and G. Senjanovic, “Neutrino Mass and Spontaneous Parity Nonconservation,” *Phys. Rev. Lett.* **44** (1980) 912.
- [7] M. Fukugita and T. Yanagida, “Baryogenesis Without Grand Unification,” *Phys. Lett. B* **174** (1986) 45–47.
- [8] S. Davidson and A. Ibarra, “A Lower bound on the right-handed neutrino mass from leptogenesis,” *Phys. Lett. B* **535** (2002) 25–32, [arXiv:hep-ph/0202239](#).
- [9] W. Buchmuller, P. Di Bari, and M. Plumacher, “Cosmic microwave background, matter - antimatter asymmetry and neutrino masses,” *Nucl. Phys. B* **643** (2002) 367–390, [arXiv:hep-ph/0205349](#). [Erratum: *Nucl. Phys. B* 793, 362 (2008)].

- [10] G. F. Giudice, A. Notari, M. Raidal, A. Riotto, and A. Strumia, “Towards a complete theory of thermal leptogenesis in the SM and MSSM,” *Nucl. Phys. B* **685** (2004) 89–149, [arXiv:hep-ph/0310123](#).
- [11] A. Zee, “A Theory of Lepton Number Violation, Neutrino Majorana Mass, and Oscillation,” *Phys. Lett. B* **93** (1980) 389. [Erratum: *Phys.Lett.B* 95, 461 (1980)].
- [12] T. P. Cheng and L.-F. Li, “Neutrino Masses, Mixings and Oscillations in SU(2) x U(1) Models of Electroweak Interactions,” *Phys. Rev. D* **22** (1980) 2860.
- [13] A. Zee, “Quantum Numbers of Majorana Neutrino Masses,” *Nucl. Phys. B* **264** (1986) 99–110.
- [14] K. S. Babu, “Model of ‘Calculable’ Majorana Neutrino Masses,” *Phys. Lett. B* **203** (1988) 132–136.
- [15] L. M. Krauss, S. Nasri, and M. Trodden, “A Model for neutrino masses and dark matter,” *Phys. Rev. D* **67** (2003) 085002, [arXiv:hep-ph/0210389](#).
- [16] E. Ma, “Verifiable radiative seesaw mechanism of neutrino mass and dark matter,” *Phys. Rev. D* **73** (2006) 077301, [arXiv:hep-ph/0601225](#).
- [17] M. Aoki, S. Kanemura, and O. Seto, “Neutrino mass, Dark Matter and Baryon Asymmetry via TeV-Scale Physics without Fine-Tuning,” *Phys. Rev. Lett.* **102** (2009) 051805, [arXiv:0807.0361 \[hep-ph\]](#).
- [18] K. Cheung and O. Seto, “Phenomenology of TeV right-handed neutrino and the dark matter model,” *Phys. Rev. D* **69** (2004) 113009, [arXiv:hep-ph/0403003](#).
- [19] A. Ahriche and S. Nasri, “Dark matter and strong electroweak phase transition in a radiative neutrino mass model,” *JCAP* **07** (2013) 035, [arXiv:1304.2055 \[hep-ph\]](#).
- [20] T. A. Chowdhury and S. Nasri, “Charged Lepton Flavor Violation in a class of Radiative Neutrino Mass Generation Models,” *Phys. Rev. D* **97** no. 7, (2018) 075042, [arXiv:1801.07199 \[hep-ph\]](#).
- [21] R. Cepedello, M. Hirsch, P. Rocha-Morán, and A. Vicente, “Minimal 3-loop neutrino mass models and charged lepton flavor violation,” *JHEP* **08** (2020) 067, [arXiv:2005.00015 \[hep-ph\]](#).
- [22] Y. Irie, O. Seto, and T. Shindou, “Lepton flavour violation in a radiative neutrino mass model with the asymmetric Yukawa structure,” *Phys. Lett. B* **820** (2021) 136486, [arXiv:2104.09628 \[hep-ph\]](#).
- [23] O. Seto, T. Shindou, and T. Tsuyuki, “Lower bounds on lepton flavor violating branching ratios in a radiative seesaw model,” *Phys. Rev. D* **105** no. 9, (2022) 095018, [arXiv:2202.00931 \[hep-ph\]](#).
- [24] M. Lindner, M. Platscher, C. E. Yaguna, and A. Merle, “Fermionic WIMPs and vacuum stability in the scotogenic model,” *Phys. Rev. D* **94** no. 11, (2016) 115027, [arXiv:1608.00577 \[hep-ph\]](#).

- [25] D. Suematsu, T. Toma, and T. Yoshida, “Reconciliation of CDM abundance and $\mu \rightarrow e \gamma$ in a radiative seesaw model,” *Phys. Rev. D* **79** (2009) 093004, [arXiv:0903.0287 \[hep-ph\]](#).
- [26] P.-H. Gu, “High-scale leptogenesis with three-loop neutrino mass generation and dark matter,” *JHEP* **04** (2017) 159, [arXiv:1611.03256 \[hep-ph\]](#).
- [27] M. D’Onofrio, K. Rummukainen, and A. Tranberg, “Sphaleron Rate in the Minimal Standard Model,” *Phys. Rev. Lett.* **113** no. 14, (2014) 141602, [arXiv:1404.3565 \[hep-ph\]](#).
- [28] “The International Linear Collider Technical Design Report - Volume 1: Executive Summary,” [arXiv:1306.6327 \[physics.acc-ph\]](#).
- [29] M. T. Núñez Pardo de Vera, M. Berggren, and J. List, “Evaluating the ILC SUSY reach in the most challenging scenario: $\tilde{\tau}$ NLSP, low ΔM , lowest cross-section,” in *2022 Snowmass Summer Study*. 3, 2022. [arXiv:2203.15729 \[hep-ph\]](#).
- [30] **CLIC accelerator** Collaboration, “The Compact Linear Collider (CLIC) - Project Implementation Plan,” [arXiv:1903.08655 \[physics.acc-ph\]](#).
- [31] **FCC** Collaboration, A. Abada *et al.*, “FCC-ee: The Lepton Collider: Future Circular Collider Conceptual Design Report Volume 2,” *Eur. Phys. J. ST* **228** no. 2, (2019) 261–623.
- [32] **CEPC Study Group** Collaboration, M. Dong *et al.*, “CEPC Conceptual Design Report: Volume 2 - Physics & Detector,” [arXiv:1811.10545 \[hep-ex\]](#).
- [33] J. Yuan, H. Cheng, and X. Zhuang, “Prospects for slepton pair production in the future e^-e^+ Higgs factories,” [arXiv:2203.10580 \[hep-ex\]](#).
- [34] E. Ma, “Common origin of neutrino mass, dark matter, and baryogenesis,” *Mod. Phys. Lett. A* **21** (2006) 1777–1782, [arXiv:hep-ph/0605180](#).
- [35] N. Haba and O. Seto, “Low scale thermal leptogenesis in neutrinophilic Higgs doublet models,” *Prog. Theor. Phys.* **125** (2011) 1155–1169, [arXiv:1102.2889 \[hep-ph\]](#).
- [36] S. Bertolini, F. Borzumati, A. Masiero, and G. Ridolfi, “Effects of supergravity induced electroweak breaking on rare B decays and mixings,” *Nucl. Phys. B* **353** (1991) 591–649.
- [37] **MEG** Collaboration, A. M. Baldini *et al.*, “Search for the lepton flavour violating decay $\mu^+ \rightarrow e^+ \gamma$ with the full dataset of the MEG experiment,” *Eur. Phys. J. C* **76** no. 8, (2016) 434, [arXiv:1605.05081 \[hep-ex\]](#).
- [38] **ALEPH** Collaboration, A. Heister *et al.*, “Search for scalar leptons in e^+e^- collisions at center-of-mass energies up to 209-GeV,” *Phys. Lett. B* **526** (2002) 206–220, [arXiv:hep-ex/0112011](#).
- [39] **ALEPH** Collaboration, A. Heister *et al.*, “Absolute mass lower limit for the lightest neutralino of the MSSM from e^+e^- data at $s^{*(1/2)}$ up to 209-GeV,” *Phys. Lett. B* **583** (2004) 247–263.

- [40] **DELPHI** Collaboration, J. Abdallah *et al.*, “Searches for supersymmetric particles in $e^+ e^-$ collisions up to 208-GeV and interpretation of the results within the MSSM,” *Eur. Phys. J. C* **31** (2003) 421–479, [arXiv:hep-ex/0311019](#).
- [41] **L3** Collaboration, P. Achard *et al.*, “Search for scalar leptons and scalar quarks at LEP,” *Phys. Lett. B* **580** (2004) 37–49, [arXiv:hep-ex/0310007](#).
- [42] **OPAL** Collaboration, G. Abbiendi *et al.*, “Search for anomalous production of dilepton events with missing transverse momentum in $e^+ e^-$ collisions at $s^{*1/2} = 183$ -GeV to 209-GeV,” *Eur. Phys. J. C* **32** (2004) 453–473, [arXiv:hep-ex/0309014](#).
- [43] **CMS** Collaboration, “Search for direct pair production of supersymmetric partners of τ leptons in the final state with two hadronically decaying τ leptons and missing transverse momentum in proton-proton collisions at $\sqrt{s} = 13$ TeV,” [arXiv:2207.02254 \[hep-ex\]](#).
- [44] LEPSUSYWG, “Aleph, delphi, l3 and opal experiments, note lepsusywg/04-01.1.” <http://lepsusy.web.cern.ch/lepsusy/Welcome.html>.
- [45] E. W. Kolb and M. S. Turner, *The Early Universe*, vol. 69. 1990.
- [46] **Belle** Collaboration, A. Abdesselam *et al.*, “Search for lepton-flavor-violating tau-lepton decays to $\ell\gamma$ at Belle,” *JHEP* **10** (2021) 19, [arXiv:2103.12994 \[hep-ex\]](#).
- [47] **Particle Data Group** Collaboration, P. A. Zyla *et al.*, “Review of Particle Physics,” *PTEP* **2020** no. 8, (2020) 083C01.
- [48] L. Covi, E. Roulet, and F. Vissani, “CP violating decays in leptogenesis scenarios,” *Phys. Lett. B* **384** (1996) 169–174, [arXiv:hep-ph/9605319](#).